Hindawi
Journal of Nanomaterials
Volume 2022, Article ID 6316716, 7 pages
https://doi.org/10.1155/2022/6316716

Research Article

Structural and Optical Properties of CdSe/CdTe Core-Shell Quantum Dots

G. Ramalingam,[1] **C. Ragupathi**,[2] **Baskaran Rangasamy**,[3] **I. Colak**,[4] **V. Vetrivelan**,[5] **Neda Poudineh**,[6] **Balasubramani Ravindran**,[7] **Soon Woong Chang**,[7] **and Robert M. Gengan**[8]

[1]*Department of Nanoscience and Technology, Science Campus, Alagappa University, Karaikudi, 630003 Tamil Nadu, India*
[2]*Department of Chemistry, Sriram College of Arts and Science, Perumalpattu, Tiruvallur, 602024, Tamilnadu, India*
[3]*Energy Storage Materials and Devices Lab, Department of Physics, School of Mathematics and Natural Sciences, The Copperbelt University, PO Box 21692, Riverside, Kitwe, Zambia*
[4]*Department of Electrical and Electronics Engineering, Nisantasi University, Istanbul, Turkey*
[5]*Department of Physics, Thanthai Periyar Government Institute of Technology, Vellore, 632002, Tamilnadu, India*
[6]*Department of Energy Systems Research, Ajou University, Suwon 16499, Republic of Korea*
[7]*Department of Environmental Energy and Engineering, Kyonggi University, Yeongtong-Gu, Suwon, Gyeonggi-Do 16227, Republic of Korea*
[8]*Department of Chemistry, Faculty of Applied Sciences, Durban University of Technology, Durban 4001, South Africa*

Correspondence should be addressed to G. Ramalingam; ramanloyola@gmail.com
and Baskaran Rangasamy; baskaran.rangasamy@cbu.ac.zm

Received 7 November 2021; Revised 25 December 2021; Accepted 30 December 2021; Published 22 January 2022

Academic Editor: Karthikeyan Sathasivam

A simple hydrothermal method is developed for the synthesis of high-quality type II core-shell CdSe/CdTe quantum dots (QDs). The XRD results reveal the formation of mixed phases of CdSe and CdTe with a grain size of 12.6 nm. SEM morphology confirms the uniformly distributed nanoscale CdSe/CdTe with no agglomeration. EDX confirms the elemental presence of Cd, Se, and Te in the compound. TEM results suggest that the size of spherical CdSe/CdTe core-shell QDs is in the range of 8~10 nm. Significant results of the SAED pattern confirm the core and shell components as CdSe and CdTe, respectively. The correlation between the synthesis procedures and the corresponding structures of the core-shell CdSe/CdTe QDs is discussed. The demonstrated monodispersed lattice structure of core-shell CdSe/CdTe QDs has excellent PL emission properties at $\lambda_{emi} \sim 585$ nm which is suitable for photovoltaic applications. The UV-Vis absorption bands at 455 nm and 560 nm confirm exciton emission due to the type II matrix of CdSe/CdTe QDs.

1. Introduction

Nanoscience and nanotechnology breakthroughs have unlocked several possibilities in various fields, including solar cell systems, photodetectors, electrical injection lasers, and optical waveguides [1]. With the rapid advancement of synthesis, characterization, and methods, scientists have discovered that combining multicomponent nanomaterials and tuning their composition profile can result in more desirable properties such as textural morphology and electrical and optical behaviour which leads to enhancement of their applications in a wide variety of fields [2, 3]. Due to the tunable architecture, nanomaterials especially the core-shell nanostructures have an impact in most of the thrust research areas in recent years. Following solar energy conversion and in conjunction with the use of heterostructures, nanostructures

give various compensations, one of which is the quick exciton dissociation. In recent years, CdSe-CdTe heterostructures have been developed to improve the integration of CdTe and selenide components in solar cell structures for the compelling benefits of a number of these desirable features [4]. However, a critical factor limiting conversion capability is going to be the rapid relaxing of high-energy excitons (photostimulated) into low-energy excitons, resulting in excess energy from their conversion to heat energy via photon emission. Another factor affecting performance is photoinduced excitons dissociating into holes and free electrons, rather than recombination [5].

In general, the efficiency of unique photovoltaic device conversion is constrained by the solar energy distribution system which is associated with the host materials' bandgap. As a result, it is critical to synthesize materials with exceptional stability, a limited size range, and significant luminous performance [6]. At the moment, core-shell nanostructures of CdTe are being developed, in which conduction of core and valence bands are generally larger (or smaller) in comparison to that of the shell. Because of the exciton dispersion of heterostructure spatial separation, nanostructures can allow access to longer wavelengths than shell materials or single-core atoms [7].

This present work deals with CdSe/CdTe core-shell-based structures of type II QDs that critically rely on their synthesis processes and are examined with traditional powder X-ray diffraction (PXRD), SEM-EDX, TEM, and SAED pattern and optical characterization (UV-Vis, PL spectrum). The correlation between the synthesis procedures and the corresponding structures of the QD for the photovoltaic and energy storage applications is discussed.

2. Experimental Section

2.1. Materials. All the chemical reagents are of analytical grade (AR) and used without any further purification. The precursors, cadmium nitrate tetrahydrate ($Cd(NO_3)_2{\cdot}4H_2O$) (Merck 99%), sodium selenite (Na_2SeO_3) (Merck 98%), sodium borohydride ($NaBH_4$) (Sigma-Aldrich, >98%), Te (Merck), hydrazine hydrate ($N_2H_4{\cdot}H_2O$) (Merck), ammonia ($NH_3{\cdot}H_2O$), sodium tetra borate ($Na_2B_4O_7$) (Sigma-Aldrich, 99%), and L-cysteine ($C_3H_7{\cdot}NO_2S$) (Sigma-Aldrich, 97%), are acquired and used for the synthesis of CdSe/CdTe quantum dots. Milli-Q water used for hydrothermal reactions is collected from Millipore Milli-Q lab water system.

2.2. Synthesis of CdSe/CdTe QDs. CdSe/CdTe QDs have been synthesized in a two-step process such that the CdSe nanoparticles are prepared separately and mixed with the precursors of CdTe in a hydrothermal process. The precursor materials used for CdSe synthesis are cadmium nitrate tetrahydrate ($Cd(NO_3)_2{\cdot}4H_2O$), sodium selenite (Na_2SeO_3), hydrazine hydrate ($N_2H_4{\cdot}H_2O$), and ammonia ($NH_3{\cdot}H_2O$). The raw materials $Cd(NO_3)_2{\cdot}4H_2O$ and Na_2SeO_3 are taken in a molar ratio of 2 : 1. The detailed synthesis procedure of CdSe nanoparticles has been carried out in a similar method as discussed in the earlier reports of the authors, Ramalingam et al. and Lin et al. [8, 9]. In order to prepare CdTe, one of the precursor materials NaHTe is freshly prepared by mixing $NaBH_4$ with Te by a 2 : 1 molar ratio dissolved in aqueous solution as mentioned in the following reaction:

$$4NaBH_4 + 2Te + 7H_2O \longrightarrow 2NaHTe + Na_2B_4O_7 + 14H_2\uparrow \quad (1)$$

Stoichiometry amounts of $NaBH_4$ (0.75 g) is transferred to a conical flask which has already been chilled with ice, followed by 10 ml of H_2O and Te (2.55 g) powder. The reaction of $NaBH_4$ with Te is shown in equation (1). After 2 hours of stirring, the black Te powder is dissolved in sodium borohydride solution. The reaction of $NaBH_4$ with Te produces sodium tetra borate ($Na_2B_4O_7$) white precipitates at the bottom of the flask along with the supernatant sodium hydrogen telluride (NaHTe). A tiny exit is linked to the flask which allows the escape of hydrogen pressure developed. The supernatant NaHTe is separated by filtration for the CdTe preparation. In order to synthesize CdSe/CdTe core-shell structured quantum dots, a repeated precursor solution addition along with an L-cysteine capping agent has been carried out. Cadmium nitrate tetrahydrate ($Cd(NO_3)_2{\cdot}4H_2O$) is dissolved in a freshly prepared NaHTe solution along with 1.2 g of L-cysteine ($C_3H_7{\cdot}NO_2S$) in 25 ml of Milli-Q water, and progressively CdSe is included. The overall reaction is shown in

$$\begin{aligned} NaHTe + Cd(NO_3)_2 4H_2O + CdSe &\xrightarrow{\text{L-Cysteine}} CdSe \\ &- CdTe{\downarrow} + NaOH + N_2O{\uparrow} + 4H_2O + 2O_2{\uparrow} \end{aligned} \quad (2)$$

The NaOH formed during the reaction could maintain the required solution pH as high as possible. The solution is shifted to a Teflon-lined autoclave and kept in an oven at 180°C for 6 hours. Figure 1 illustrates a step-by-step process of the CdSe/CdTe quantum dot synthesis process. As illustrated in Figure 1, as the first step, the cadmium nitrate tetrahydrate and sodium selenite are dissolved in double-distilled water separately. The dissociated Cd^{2+} ion in cadmium nitrate solution is turned into $Cd(NH_3)_4^{2+}$ complex ion when treated with ammonia. On the other hand, the Se source Na_2SeO_3 is dissociated when mixed with hydrazine hydrate, and subsequently hydrogen selenide (H_2Se) is formed in which the oxidation state of selenium changes to Se^{2-}. A CdSe cluster is formed when both of these Cd and Se solutions are mixed together which is then added to the precursor solution of CdTe as mentioned above. The ligand molecules of CdTe are bound with the CdSe surface to produce CdSe-wrapped CdTe quantum dots under hydrothermal treatment at 180°C as depicted in Figure 1.

After cooling down the hydrothermal reactor, the resulting solution is then transferred to a refluxing conical flask and heated to 110°C under refluxing in different duration to control the size of CdSe/CdTe QDs. The resultant solution is then centrifuged, and the precipitates are extracted through filtration. The precipitates are repeatedly washed with Milli-Q water and ethanol in order to remove traces of NaOH and impurities if any. The precipitates are

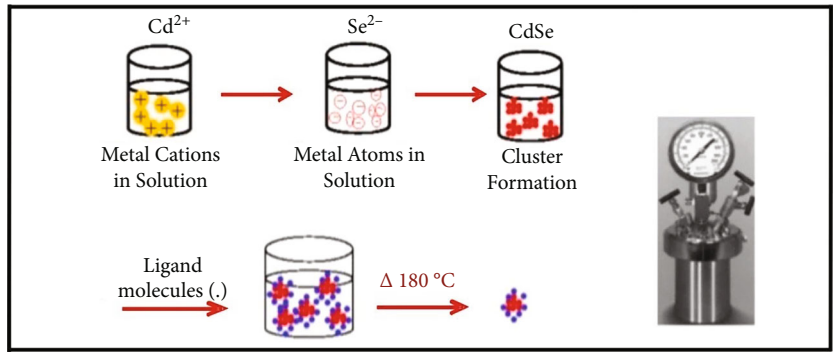

Figure 1: Schematic diagram of synthesis of CdSe/CdTe quantum dots.

extracted through vacuum suction filtration followed by heat treatment at 110°C for three hours. After heat treatment, a deep crimson CdSe/CdTe powder sample is obtained. The final powder is investigated by XRD, SEM-EDX, TEM, and SAED to confirm the formation of nanoscale CdSe/CdTe core-shell structure.

2.3. Characterization Techniques. The powder XRD patterns of the as-prepared nanocomposites are documented on a rich SEIFER alongside nickel-filtered (monochromatic) CuKα radiation of 1.5406 Å with a 0.02°/sec scanning rate. A JEOL Scanning Electron Microscope (SEM) at 10 kV along with EDX (energy-dispersive X-ray analyzer) (JSM 6310) is used for investigating the morphology of the nanostructured materials. A Transmission Electron Microscope (TEM) (JEOL-JEM 2010) with a 200 kV acceleration voltage is used to capture microscopic images of nanostructures. All samples are cleaned using hexanes, methanol extraction, and acetone precipitation. Copper grids covered with an ultrathin carbon film or formvar film are dipped into a toluene or hexane solution. A 120 cm camera is used to record "SAED (selected area electron diffraction patterns)." The absorption spectrum is acquired using a UV-Vis-NIR spectrometer in the 200 nm to 900 nm range (CARY 5E double beam). The emission spectrum is recorded using a spectrophotometer (FLOUROLET-3) in a spectral range of 300 nm to 600 nm with a xenon lamp with 380 nm excitation wavelength as a source.

3. Results and Discussion

3.1. Powder X-Ray Diffraction (XRD). The as-prepared CdSe/CdTe compound is characterized by powder XRD, and the corresponding XRD pattern is shown in Figure 2. The diffraction peaks observed at 24.19°, 27.62°, 42.28°, and 56.95° are ascribed to the planes (002), (101), (112), and (002), respectively, which reveals CdSe hexagonal phase formation. The diffraction peaks observed at 13.70°, 24.19°, 35.38°, and 39.87° are assigned to the planes (100), (111), (211), and (220) of the CdTe cubic phase, respectively. The characteristic peaks indicate the formation of the hexagonal CdSe and cubic CdTe polycrystalline compound. The diffraction peaks are of best match with JCPDS card no. 77-2304 and JCPDS card no. 89-3011 corresponding to CdTe

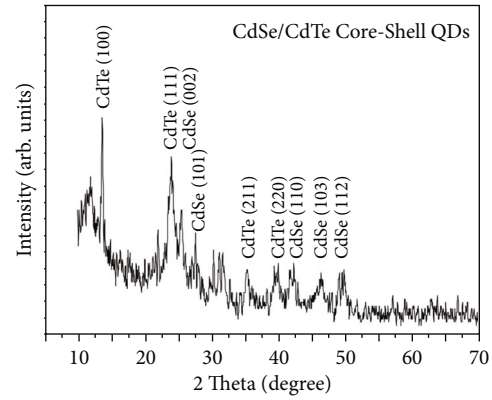

Figure 2: The X-ray powder diffraction patterns of CdSe/CdTe core-shell quantum dots.

and CdSe, respectively. The signatures of diffraction peaks are wider because of the constrained particle size. Though the CdSe is wrapped by CdTe, the diffraction peaks corresponding to the cubic structure of CdSe are revealed [8].

The crystallite size as well as the induced strain is calculated by the Williamson-Hall method [10] as per

$$\beta \cos \theta = \frac{K\lambda}{D} + 4\varepsilon \sin \theta, \quad (3)$$

where β is the full width at half maximum of the intensity (FWHM), θ is Bragg's angle, K is the shape factor which could be used as 0.9, λ is the wavelength of the X-ray used, D is the crystallite size, and ε represents the strain. The grain size of CdSe/CdTe is found to be 12.6 nm by using the Williamson-Hall formula which indicates quantum dot (QD) formation. The unique nature of QD nanocrystals lies in the size of the particle and coordinated shape. In order to understand the shape and presence of elements, SEM-EDX and TEM measurements are carried out.

3.2. SEM-EDX Analysis. Figure 3(a) shows the SEM image of CdSe/CdTe nanoparticles. The surface morphology indicates uniform particle size distribution of CdSe/CdTe nanoparticles throughout the surface. The spherical nanoparticles are monodispersed without agglomeration. The surface view reveals circular shapes of the nanoparticles with particle

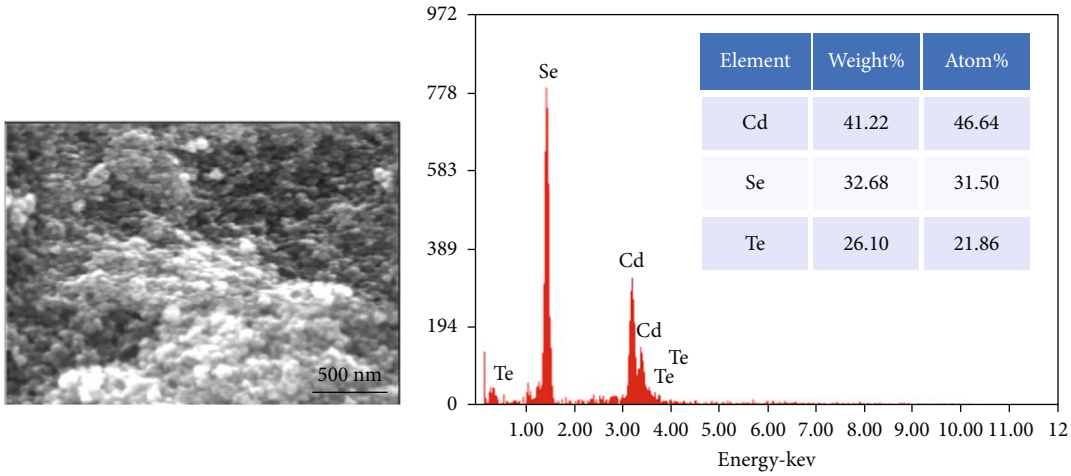

Figure 3: (a) SEM morphology and (b) EDX spectrum of CdSe/CdTe.

sizes in the range of 10~20 nm. However, the size of QDs is not precisely determined from SEM morphology for which TEM analysis is performed. The EDS spectrum of CdSe/CdTe indicates the presence of Cd, Se, and Te elements as shown in Figure 3(b). The atomic and weight percentage of Cd is high which reveals the presence of Cd bonding with both Se and Te as in CdSe and CdTe compounds.

3.3. TEM Analysis. The size and shape of QDs are investigated by using TEM imaging. Nonetheless, due to the presence of a fuzzy projection of the thin shell and to justify the lower contrast of electron density between the shell and core atmosphere, a vivid core-shell nanostructure illustrated by TEM images is reported by Sheu et al. [11]. In order to realize the particle size and shape of QDs, an effort is made to observe TEM morphology. The TEM images observed for CdSe/CdTe nanostructures are shown in Figures 4(a)–4(e). The TEM images observed at the 50-100 nm scale indicate extraordinarily highly monodispersive and spherical-shaped nanoparticles as shown in Figures 4(a) and 4(b). Further magnifications to the 20 nm scale as shown in Figure 4(c) reveal the most precise particle size in the order of 8~10 nm sized quantum dots which is in concurrence with XRD and SEM results.

The TEM morphology at higher magnifications also exemplifies freestanding particle dispersion without any agglomerates which is in good agreement with SEM morphology results. It is interesting to note that the as-prepared CdSe/CdTe nanostructures are found without any agglomeration which is naturally detected while using most of the alternative solvents. During the synthesis of CdSe/CdTe, L-cysteine is used as a capping agent which plays a major role in tuning the size of QDs and alleviating the agglomeration by producing freestanding nanoarchitectures [8, 9]. In order to reveal the core-shell structure of the CdSe/CdTe compound, further magnifications are performed at the particle level scale. On very high magnifications at 5 nm scales, the particle surface shows a merging of two different crystal structures which might be corresponding to CdSe QDs surrounded with CdTe QD patches as shown in Figures 4(d) and 4(e).

The surface of CdSe and wrapping compound CdTe are indicated in circles in Figure 4(d). A mixed crystal phased regions are apparently evidenced in Figure 4(e) which reveals the presence of two different crystal structures in the compound. The TEM results at higher magnifications significantly at the 5 nm scale clearly evidence the core-shell structure of CdSe/CdTe quantum dots. The CdSe QDs are bound with the top layer CdTe in a heterojunction that forms an excellent core-shell structure as confirmed by TEM morphology.

The heterojunction core-shell structured QDs offer significantly more impacts on photovoltaic applications. When combined with effective exciton production and dissociation, they result in discrete channels for the transport of separated charge carriers [9]. It is now practically possible to construct heterojunction core-shell QDs with control at the atomic level over the core and shell positions as well as the composites throughout the interface using current colloidal chemistry techniques combined with a hydrothermal method. As a result, new routes to identify high or effective luminescence materials for photovoltaic device application have been unlocked [12]. In order to clarify the core and shell components, the SAED pattern is observed at a selected region as shown in Figure 4(f). The SAED pattern depicts two regions with different crystal structures. The inner circle region is attributed to the (002) plane of CdSe, and the outer circle region is attributed to the (100) plane of CdTe. The remarkable SAED pattern results evidently reveal the mixture of crystal phases corresponding to CdSe as a core and CdTe as a shell in the core-shell structured QDs. A schematic representation of core-shell structured CdSe/CdTe growth orientation and electron-hole trapping at the interface in the core-shell structure is demonstrated in Figures 5(a) and 5(b)).

The nonpolar interfaces $(10\bar{1}0)$ of the surface facet are guided towards the wurtzite (0001) direction as shown in Figure 5(a). At the interface of the core-shell structure, a

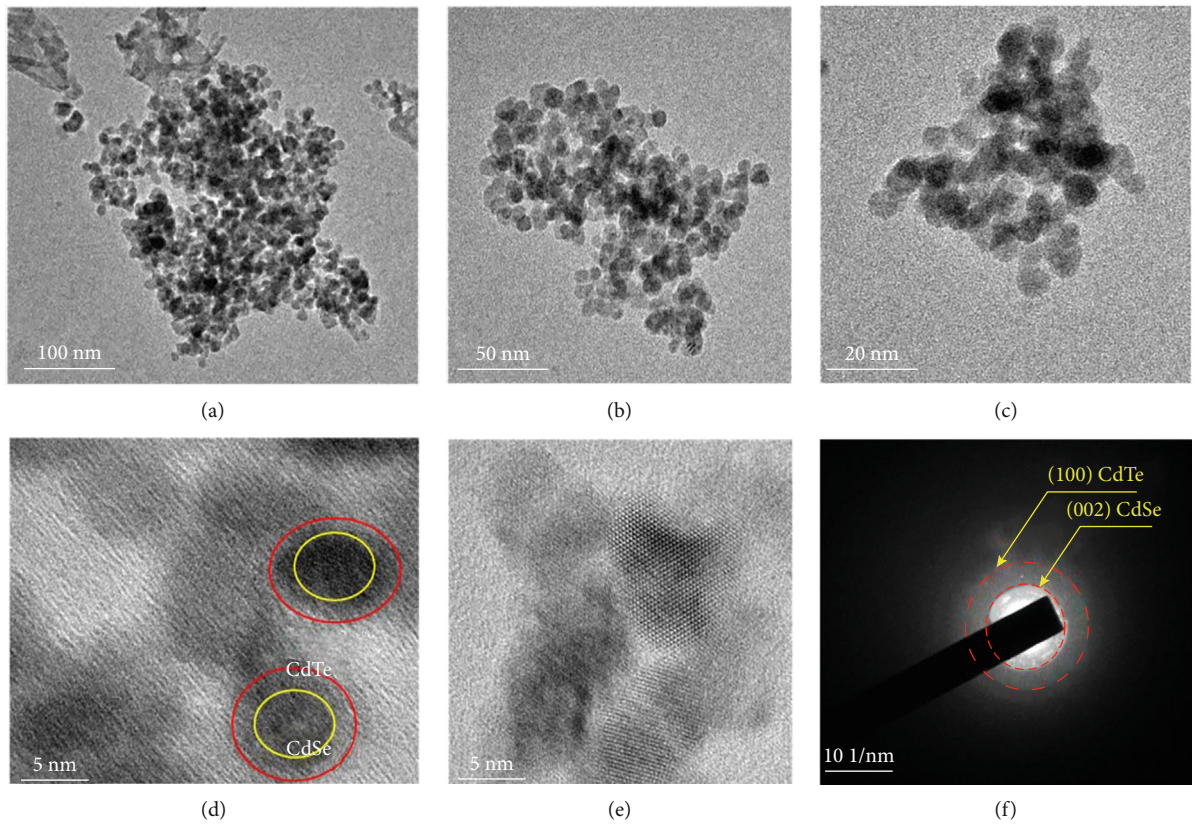

Figure 4: (a–e) TEM images and (f) SAED pattern of CdSe/CdTe core-shell quantum dots.

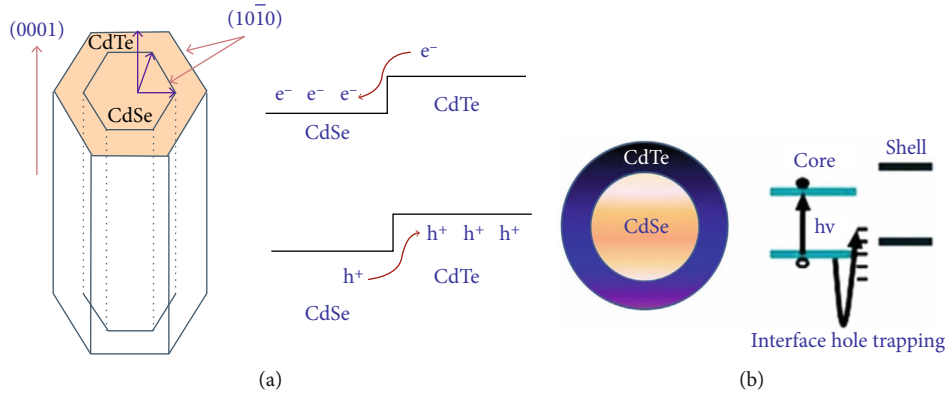

Figure 5: Schematic representation of CdSe/CdTe (a) growth orientation and (b) electron-hole trapping in the core-shell structure.

fraction of holes are trapped. The trapped holes at the interface might be acting as a cracking site or electron-hole recombination. It is predicted to be a dangling bond defect which is related to the defect centre due to the cracking site process and as a least possibility of which may be a recombination centre as illustrated in Figure 5(b). As discussed in TEM analysis, due to a significant lattice mismatch among many core-shell nanoparticle locations, a substantially less uniaxial pressure is required which could be due to the influence of band offsets or bandgap throughout the surface [13].

3.4. Nucleation Growth Mechanism. High-quality monodispersive quantum dots have been reported extensively; however, the following KHSe or NaHSe reagents have produced broadly with the source of "Se" as the Na_2SeO_3 compound that has been condensed by sodium borohydride ($NaBH_4$) at normal reaction conditions to create Se^{2-} [14]. In the present work, hydrogen selenide (H_2Se) and sodium hydrogen telluride (NaTeH) are used as reagents along with cadmium nitrate for CdSe and CdTe, respectively. The reaction has been performed in an open-air condition which makes the process easier and less time-consuming. The nucleation growth followed

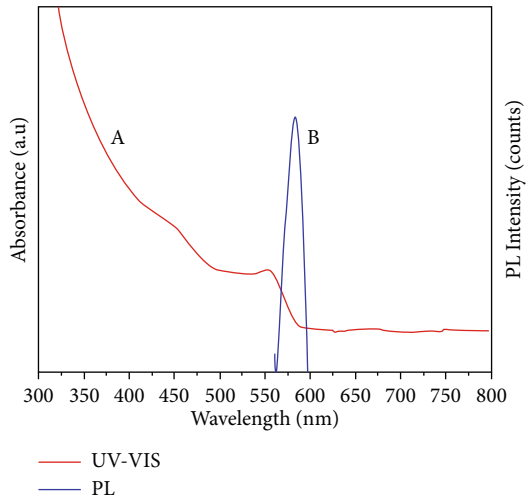

Figure 6: (a) Optical absorption and (b) photoluminescence spectrum of CdSe/CdTe core-shell quantum dots.

by a larger enhancement at higher temperature may increase the quantum efficiency and possible growth mechanism. The surface and interface nature of the CdSe/CdTe core-shell quantum dots may have the available source of interactions between the interfacial charge-carrier boundaries which are caused by trapping due to the variance of lattice direction [15]. The defects of the interface of the CdSe/CdTe core-shell quantum dots are due to the greater variance between lattices and impact of graded interfaces. In our knowledge, the graded core-shell creation could perhaps have multifolded benefits such as (i) possible production of defects at the interface and (ii) generation of variance in energy bands that could enhance charge transfer flowing across the interface that leads the internal electric field. The band alignment creates tunnelling of charge carriers across the interface of the core-shell structure. The schematic diagram displays a charge transfer mechanism using core-shell activities along with the reverse path of electron-hole recombination in the CdSe/CdTe QDs [16].

3.5. Optical Absorption and Photoluminescence Properties. Figure 6 shows both emission and absorption spectra of CdSe/CdTe QDs. The UV-visible absorption spectrum of CdSe/CdTe QDs has been recorded in the 200 nm to 800 nm spectral range. The CdSe/CdTe QDs shows an excitonic peak at 560 nm as shown in Figure 6(a). On the other hand, Figure 6(b) suggests the monodispersed CdSe/CdTe QDs and narrow size distribution of PL emission spectra at $\lambda_{emi} \sim 585$ nm which indicates emission near the band edge. Moreover, it is indicated that there is an increase in emission due to HOMO and LUMO charge carriers implying direct recombination when PL emission spectral maximum lies closer to its absorption onset [17]. The absorption spectrum of CdSe/CdTe QDs indicates a formation of type II core-shell nanostructure characteristics. Therefore, the charge spatial separation transport of quantum yield reduction is because of wave function (focused) coverage among holes trapped at the shell surface and localized electrons at the heterostructure matrix. The UV-Vis absorption band at 455 nm and a broad band at 560 nm along with a PL emission peak at 585 nm indicate exciton emission of the type II matrix which has a wider band due to the trapping mode as observed in emission spectra [18].

The emission observed in the $\lambda_{emi} \sim 560$-590 nm wide regions is resulted by the existence of several structural defects in the synthesized CdSe/CdTe material. The possible reason for visible emission may be due to the surface to volume (s/v) substantial ratio that resulted in creating interstitials as well as vacancies (high-density surface defects) which can cause a trap level. The nature of defects and dopants at grain boundary leads to decreasing free carrier movement and bulk counterpart surface [19].

Even though free carriers are scattered when in contact with charged dopants or closer defects, there is a possible decrease in mobility which restricts carrier separation [20]. In this context, the CdTe doping at low concentration results in the development of radiative recombination with extra centres at the CdSe which leads to the improvement in photoluminescence emission intensity. The graded core-shell formation offers a multifold benefit as evidenced from UV-Vis and PL emission spectral analyses. Based on the optical properties, three different arguments are categorized such as (i) band alignment experiences at the heterointerfaces with a lesser amount of strain at the graded core-shell in comparison with ungraded conditions, (ii) a decrease in defect locations at the interface, and (iii) the positioning ending up with cascading of charge transfer locally. These factors of CdSe/CdTe core-shell structured QDs contribute greatly to enhancing the yield of charge separation and charge carrier mechanism which might have an effect on the photovoltaic device efficiency enhancements. The uniform spherical core-shell structured CdSe/CdTe QDs with excellent size and shape properties could be utilized as an electrode in energy storage applications which may have excellent electrochemical properties.

4. Conclusions

In summary, the particular work emphasizes a controlled synthesis of core-shell structured CdSe/CdTe quantum dots by a colloidal chemistry approach equipped with the hydrothermal technique. The CdSe/CdTe compound has been investigated by powder XRD which reveals the mixture phase polycrystalline hexagonal CdSe and cubic CdTe formation. The grain size determined from XRD results by the Williamson-Hall method indicates 12.6 nm. The SEM morphology indicates uniform monodispersed spherical nanoscale particles of CdSe/CdTe. The EDX confirms the presence of Cd, Se, and Te in the CdSe/CdTe compound. TEM investigations confirm the spherical-shaped core-shell structured quantum dots and precise particle sizes ranging between 8 and 10 nm which is in good agreement with XRD and SEM results. The SAED analysis of CdSe/CdTe confirms the core and shell components as CdSe and CdTe, respectively, which significantly proves the core-shell structure elements. With the existence of an absorbance characteristic, the SAED pattern that approximated the core-shell

QDs combined with wurtzite zinc-blended structures reveals a weak quantum confinement effect of charges. The intensity of PL emission at $\lambda_{emi} \sim 585$ nm is found to be high in the synthesized CdSe/CdTe core-shell QDs indicating the type II heterostructured matrix. In nutshell, the proposed novel strategy of tunable CdSe/CdTe core-shell QDs with excellent structure, size and shape, morphology, and optical properties is suitable for photovoltaic and energy storage applications.

Data Availability

The composition data will be available based on request.

Conflicts of Interest

The authors declare that they have no conflicts of interest regarding the publication of this paper.

Acknowledgments

One of the corresponding authors, Dr. G. Ramalingam, gratefully acknowledges the Rashtriya Uchchatar Shiksha Abhiyan (RUSA) 2.0 award no. F.24-51/2014-U (Policy (TN-Multi-Gen)), Government of India Project, for the financial support to complete this research work.

References

[1] J. C. Johnson, H. J. Choi, K. P. Knutsen, R. D. Schaller, P. Yang, and R. J. Saykally, "Single gallium nitride nanowire lasers," *Nature Materials*, vol. 1, pp. 106–110, 2002.

[2] X. Duan, Y. Huang, R. Agarwal, and C. M. Lieber, "Single-nanowire electrically driven lasers," *Nature*, vol. 5, pp. 421–425, 2003.

[3] J. S. Jie, W. J. Zhang, Y. Jiang, X. M. Meng, Y. Q. Li, and S. T. Lee, "Photoconductive characteristics of single-crystal CdS nanoribbons," *Nano Letters*, vol. 6, pp. 1887–1892, 2006.

[4] J. Tang, Z. Huo, S. Brittman, H. Gao, and P. Yang, "Solution-processed core-shell nanowires for efficient photovoltaic cells," *Nature Nanotechnology*, vol. 6, pp. 568–572, 2011.

[5] H. McDaniel, P. E. Heil, C. L. Tsai, K. Kim, and M. Shim, "Integration of type II nanorod heterostructures into photovoltaics," *ACS Nano*, vol. 5, pp. 7677–7683, 2011.

[6] A. J. Nozik, "Exciton multiplication and relaxation dynamics in quantum dots: applications to ultrahigh-efficiency solar photon conversion," *Inorganic Chemistry*, vol. 44, pp. 6893–6899, 2005.

[7] P. Wurfel, *Physics of solar cells: from principles to new concepts*, WILEY-VCH Verlag GmbH & Co. KGaA, 2005.

[8] G. Ramalingam, N. Melikechi, P. D. Christy, S. Selvakumar, and P. Sagayaraj, "Structural and optical property studies of CdSe crystalline nanorods synthesized by a solvothermal method," *Journal of Crystal Growth*, vol. 311, pp. 3138–3142, 2009.

[9] Z. Lin, S. Cui, H. Zhang et al., "Studies on quantum dots synthesized in aqueous solution for biological labelling via electrostatic interaction," *Analytical Biochemistry*, vol. 319, pp. 239–243, 2003.

[10] V. D. Mote, Y. Purushotham, and B. N. Dole, "Williamson-Hall analysis in estimation of lattice strain in nanometer-sized ZnO particles," *Journal of Theoretical and Applied Physics*, vol. 6, no. 6, pp. 1–8, 2012.

[11] H. S. Sheu, U. S. Jeng, W. J. Shih et al., "Phase separation inside the CdTe-CdSe type II quantum dots revealed by synchrotron X-ray diffraction and scattering," *Journal of Physical Chemistry C*, vol. 112, pp. 9617–9622, 2008.

[12] X. Zhong, M. Han, Z. Dong, T. J. White, and W. Knoll, "Composition-tunable $Zn_xCd_{1-x}Se$ nanocrystals with high luminescence and stability," *Journal of the American Chemical Society*, vol. 125, pp. 8589–8594, 2003.

[13] S. A. Ivanov, A. Piryatinski, J. Nanda et al., "Type-II core/shell CdS/ZnSe nanocrystals: synthesis, electronic structures, and spectroscopic properties," *Journal of the American Chemical Society*, vol. 129, pp. 11708–11719, 2007.

[14] S. Kumar and T. Nann, "Shape control of II-VI semiconductor nanomaterials," *Small*, vol. 2, pp. 316–329, 2006.

[15] P. Reiss, M. Protière, and L. Li, "Core/shell semiconductor nanocrystals," *Small*, vol. 5, no. 2, pp. 154–168, 2009.

[16] J. D. Beach and B. E. McCandless, "Materials challenges for CdTe and $CuInSe_2$ photovoltaics," *MRS Bull*, vol. 32, pp. 225–229, 2007.

[17] S. Kaniyankandy, S. Rawalekar, and H. N. Ghosh, "Charge carrier cascade in type II CdSe-CdTe graded core-shell interface," *Journal of Materials Chemistry C*, vol. 1, pp. 2755–2763, 2013.

[18] K. Wu, Q. Li, and Y. Jia, "Efficient and ultrafast formation of long-lived charge-transfer exciton state in atomically thin cadmium selenide/cadmium telluride type-II heteronanosheets," *ACS Nano*, vol. 9, pp. 961–968, 2015.

[19] A. R. Kortan, R. Hull, and R. L. Opila, "Nucleation and growth of CdSe on ZnS quantum crystallite seeds, and vice versa, in inverse micelle media," *Journal of the American Chemical Society*, vol. 112, pp. 1327–1332, 1990.

[20] S. F. Wuister, C. De Mello Donegá, and A. Meijerink, "Influence of thiol capping on the exciton luminescence and decay kinetics of CdTe and CdSe quantum dots," *The Journal of Physical Chemistry. B*, vol. 108, pp. 17393–17397, 2004.